Laser spectroscopic study on the conformations and the hydrated structures of benzo-18-crown-6-ether and dibenzo-18-crown-6-ether in supersonic jets

Ryoji Kusaka, Yoshiya Inokuchi* and Takayuki Ebata*

Department of Chemistry, Faculty of Science, Hiroshima University,
Higashi-Hiroshima 739-8526, Japan

Abstract

The laser-induced fluorescence spectra of jet-cooled benzo-18-crown-6 (B18C6) and dibenzo-18-crown-6 (DB18C6) exhibit a number of vibronic bands in the 35000–37000 cm^{-1} region. We attribute these bands to monomers and hydrated clusters by fluorescence-detected IR-UV and UV-UV double resonance spectroscopy. We found four and two conformers for bare B18C6 and DB18C6, and hydration of one water molecule reduces the number of isomers to three and one for B18C6-$(H_2O)_1$ and DB18C6-$(H_2O)_1$. IR-UV spectra of B18C6-$(H_2O)_1$ and DB18C6-$(H_2O)_1$ suggest that all isomers of the monohydrated clusters have a double proton-donor type (bidentate) hydration. That is, the water molecule is bonded to B18C6 or DB18C6 via two O–H···O hydrogen bonds. The blue shift of the electronic origin of the monohydrated clusters and quantum chemical calculation suggest that the water molecule in B18C6-$(H_2O)_1$ and DB18C6-$(H_2O)_1$ prefers to be bonded to the ether oxygen atoms near the benzene ring.

1. Introduction

Macrocyclic crown ethers are well-known molecules in host-guest chemistry.[1] The importance of these ethers originates from their remarkable selectivity in encapsulation of guest species. Efficient capture of a guest species can easily be achieved by use of appropriate ethers whose cavity size is similar to that of the guest. On the other hand, crown ethers change their conformations, and adjust the size and anisotropy of the cavity to accept various kinds of guests. In addition, conformations of crown ethers are highly affected by their environment. Up to now, studies on conformation and encapsulation of crown ethers have been carried out mostly in liquid phase by various kinds of measurements such as elementary analysis, mass spectrometry, optical absorption spectroscopy, and NMR spectroscopy.[2] From a microscopic point of view, however, these measurements only show averaged aspects of crown ethers, which is inherent in condensed phase. For the investigation of intrinsic nature of the encapsulation, one has to focus an attention on the weak intermolecular interaction that highly controls encapsulation. Jet-cooled spectroscopy, which is our present approach, seems to be ideal for the present purposes.

Target crown ethers in this study are benzo-18-crown-6 (B18C6) and dibenzo-18-crown-6 (DB18C6) (SCHEME 1). (It should be noted that the numbering of the atoms of the ether rings is different for B18C6 and DB18C6.) DB18C6 is the first crown ether that Pedersen synthesized in 1967.[3] Crown ethers having aromatic rings show quite interesting functions in encapsulation. For example, one kind of aromatic crown ethers emits strong fluorescence as a result of the capture of cations.[4] Another ether molecule changes the wavelength of the fluorescence depending on the kind of captured cations.[5] As the first step toward understanding host-guest chemistry

of crown ethers in the molecular level, we investigate conformation and hydration of B18C6 and DB18C6 in the gas phase. We apply laser-induced fluorescence (LIF) spectroscopy, UV-UV hole-burning spectroscopy and IR-UV double-resonance spectroscopy to jet-cooled B18C6 and DB18C6. In parallel, we perform quantum chemical calculation to obtain probable structures and their IR spectra. Based on the spectroscopic information and calculation results, we discuss the structure of B18C6, DB18C6 and their hydrated clusters.

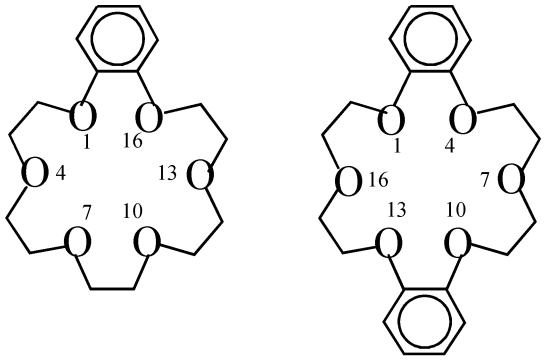

B18C6 DB18C6

SCHEME 1

2. Experimental and computational

Details of the experiment were described in our previous papers.[6] In brief, we used a home-made pulsed nozzle to generate jet-cooled B18C6 and DB18C6. This nozzle is made of poly-imido resin and suitable for getting vapor of solid samples without thermal decomposition. B18C6 or DB18C6 powder (Tokyo Kasei Kogyo) was heated to ~350 K in the pulsed nozzle. B18C6 or DB18C6 vapor was injected into a vacuum chamber with He carrier gas at a total pressure of 2 bar. B18C6 and DB18C6 samples were used without further purification.

For LIF spectroscopy, an output of a tunable pulsed UV laser (Inrad, Autotracker II (KDP)/ Lambda Physik, Scanmate/ Continuum, Surelite II) was introduced to the vacuum chamber, and crossed with the jet at ~30 mm downstream of the nozzle. Emission from the sample was collected by a series of lenses and detected by a photomultiplier tube (Hamamatsu Photonics, 1P28). For removing scattered light, a long-pass filter was placed between the lenses and the photomultiplier tube. Current from the photomultiplier tube was fed into a boxcar averager (Stanford Research Systems, SR250). The averaged signals were processed by a PC through an analog/digital converter (Stanford Research Systems, SR245) and the GPIB interface. For UV-UV hole-burning and IR-UV double-resonance spectroscopy, the same detection system was used for the probe. The frequency of the probe UV laser was fixed to the position of a vibronic band in LIF spectra for monitoring population of a specific species. For UV-UV hole-burning spectroscopy, an output of another tunable UV laser (Inrad, Autotracker II (KDP)/ Continuum, ND6000/ Continuum, Surelite II) was introduced as a UV pump laser. The UV pump laser crosses the jet at ~10 mm upstream of the probe UV laser position, which corresponds to the time interval of ~1

μs between the pump and probe pulses. The frequency of the UV pump laser was scanned while monitoring fluorescence. When the pump laser frequency was resonant to a transition of the monitored species, depletion of the fluorescence was observed. UV-UV hole-burning spectra were obtained as a function of the pump UV laser frequency. IR-UV spectra were measured with an experimental scheme similar to that of the UV-UV experiment. An output of a tunable IR laser (LaserVision/ Quanta-Ray, GCR250) was coaxially introduced with the UV probe laser 50 ns prior to the probe pulse. The frequency of the IR pump laser was scanned while monitoring the fluorescence signal. Depletion of the fluorescence occurs when the IR frequency is resonant to a vibrational transition of the monitored species. IR spectra in the S_0 state were obtained as a function of the IR frequency.

Quantum chemical calculations were carried out for B18C6, B18C6-$(H_2O)_1$, DB18C6 and DB18C6-$(H_2O)_1$. Geometry optimization and vibrational analysis were done at the B3LYP/6-31+G* level of theory. All calculations were performed by using GAUSSIAN 03.[7] We applied a scaling factor of 0.9744 to vibrational frequencies calculated. The factor was determined so as to reproduce the frequency of the OH stretching vibration of phenol monomer.[6]

3. Results and discussion

3.1. LIF spectra of B18C6 and DB18C6

Figure 1 shows the LIF spectra of jet-cooled B18C6 and DB18C6. B18C6 and DB18C6 show absorption in the similar frequency region of 35100–36900 cm^{-1}. We measured LIF spectra down to 34900 cm^{-1} for both species and found no band. This result implies that an intramolecular interaction between the two aromatic rings such as the exchange interaction is very weak in DB18C6.[8] The spectra in Fig. 1 display a group of strong bands in the 35600–35900 cm^{-1} region, and intense vibronic bands in the region higher than ~36100 cm^{-1}. At present, we cannot give conclusive assignment for all the bands in Fig. 1, since we do not observe dispersed fluorescence spectra. However, one can ascribe the vibronic bands in the 35600–35900 cm^{-1} region to the origin bands and low-frequency vibronic bands of the conformers of B18C6 or DB18C6. The bands in the region higher than 36100 cm^{-1} are probably attributed to vibronic bands of aromatic rings, because the interval between these two groups (~500 cm^{-1}) is comparable to that of mode 6b of toluene in the S_1 state (530.4 cm^{-1}).[9] To identify the number and structure of conformers, we apply UV-UV and IR-UV double-resonance spectroscopy to bands in the 35100–36000 cm^{-1} region.

3.2. Hydration of B18C6

As seen in Fig. 1a, the LIF spectrum of B18C6 displays complicated vibronic structures even in the origin band region. The main reason of the congestion is coexistence of several isomers of bare molecules as well as their hydrated clusters. In order to examine the existence of vibronic bands of hydrated clusters in the LIF

spectrum, we added a small amount of water vapor to the sample gas by passing He carrier gas on the surface of ice at 253 K. Figure 2 displays comparison of LIF spectra of B18C6 observed under different water vapor conditions. Bands marked by dots can be assigned to conformers of the B18C6 monomer. The assignment was confirmed by their IR-UV spectra, because they explicit no OH stretching band. In addition, we performed UV-UV hole-burning spectroscopy by fixing the probe frequencies to these bands, which are also shown in Figs. 2c–f. As seen in the figures, the hole-burning spectra show different dip positions for different probe bands. Thus, we conclude that there are at least four conformers of B18C6 under our experimental condition. Table 1 lists the positions of the S_1–S_0 origin bands.

Since bands marked by A, B, C and asterisks still remain strong upon the addition of water, these bands are due to hydrated clusters. To determine the size and the structure of hydrated clusters, we observed IR-UV spectra by monitoring these bands. Figure 3 shows fluorescence-detected IR dip spectra observed by monitoring bands A, B and C. Since these IR spectra exhibit two OH bands in the 3200–3750 cm^{-1} region, bands A, B and C are assigned to the B18C6-$(H_2O)_1$ cluster. IR-UV spectra observed by monitoring the bands marked by asterisks show more than two bands in the OH stretching region, though they are not shown here. Therefore, the vibronic bands marked by asterisks in Fig. 2 are ascribed to B18C6-$(H_2O)_n$ clusters with $n > 1$. The analysis of higher size clusters will be given elsewhere. Since the cluster bands appear both in Figs. 2a and 2b, it is concluded that the gas sample already contained some residual water without addition of water vapor.

The IR spectra in Fig. 3 show characteristic hydration features of B18C6-$(H_2O)_1$. First is that since the three spectra show different OH stretching

frequencies, they belong to different isomers. Second is that the IR spectra have no absorption around 3700 cm^{-1}, which means no free OH group in these clusters. Ohno and co-workers investigated hydration of short-chain poly(oxyethylene)s in CCl_4 solution by IR spectroscopy.[10] They suggested that some of hydrated poly(oxyethylene)s have a double proton-donor type (bidentate) hydrogen bond; that is, both OH groups of one water molecule are bonded to oxygen atoms of poly(oxyethylene)s. The symmetric and asymmetric OH stretching vibrations of such a bidentate water appear at 3525 and ~3590 cm^{-1}, respectively. IR intensities of these bands are almost the same as each other. From these findings, we assign the two IR bands in Fig. 3 to the symmetric and asymmetric OH stretch vibrations of B18C6-$(H_2O)_1$ with a bidentate hydration.

According to reports on hydration of poly(oxyethylene)s and crown ethers in the liquid phase,[10, 11] water molecules are bonded to the ether oxygen atoms as a donor, and there is another restriction for the bidentate hydration to these ethers. Ohno and co-workers found that the bidentate solvation of a water molecule does not occur to neighboring oxygen atoms, which are directly connected by the $–CH_2–CH_2–$ frame.[10] They explained this structural constraint by unfavorable dipole-dipole interaction between the $–O–CH_2–CH_2–O–$ frame and a water molecule. This constraint was held in hydration to 1,2-dimethoyethane ($CH_3–O–CH_2–CH_2–O–CH_3$), for which only the single proton-donor type (monodentate) hydration occurs.[12] A similar structural limitation is seen in hydration of 1,2-dimethoxybenzene (DMB) in the gas phase. Pratt and co-workers reported rotationally-resolved electronic spectra of the DMB monomer and the DMB-$(H_2O)_1$ cluster.[13] The DMB monomer has a planar heavy-atom structure with trans-disposed methoxy groups. In the case of the DMB-$(H_2O)_1$ complex, the

water molecule is attached via two O–H···O hydrogen bonds to the methoxy groups. However, the molecular plane of the water molecule is largely tilted from the plane of the DMB aromatic ring. Apparently, this hydration is not so strong because all the O–H···O atoms in the hydrogen bonds do not lie on the same line and the displacement is quite large. This type of hydration seems not to be suitable for crown ethers, because the oxygen atom of the water molecule would be located near the oxygen atoms of crown ethers, inducing oxygen-oxygen repulsion. Rather, the B18C6-$(H_2O)_1$ complex is thought to have a double O–H···O hydrogen bonds between the water molecule and the ether oxygen atoms that are not neighbors to each other.

The position of the origin bands in the LIF spectra also gives some insight into the hydration structure of B18C6-$(H_2O)_1$. Methoxybenzene (MB) monomer has the origin band of the S_1–S_0 transition at 36386 cm^{-1},[14] while that of DMB appears at 35751 cm^{-1}. Thus, the substitution of one methoxy group to MB shifts the origin band to the lower frequency by 635 cm^{-1}.[13] As shown by Pratt and co-workers, the highest-occupied molecular orbital (HOMO) of DMB largely extends towards the two oxygen atoms.[13] Therefore, with the increase of the delocalization of the HOMO orbital to the oxygen atoms, the frequency of the origin band becomes lower. For DMB, the degree of the HOMO delocalization can be maximized by locating all the atoms of –C–O–C–C–O–C– frame (the middle two carbon atoms participate in the benzene ring, and the end carbon atoms are a part of the methyl groups) on the same plane. Among the monomer origins of B18C6 in Fig. 2, the 35167 cm^{-1} band is largely apart from the other bands around 35640 cm^{-1}. This result suggests that the monomer conformation providing the 35167 cm^{-1} band has more planar nature around the benzene ring than those of the other monomer conformations. Another possibility

is that this band is due to a species different from B18C6. Though we cannot deny completely this possibility, the similarity of the blue shift due to the hydration (band A) as well as the IR spectrum of this hydrated cluster strongly suggests that this species is due to the one of the conformers of B18C6. This discussion will be given in the next. It should be noted that such the larger difference of the electronic transitions for different conformers is also reported N-acetyl tryptophane methyl amide (NATMA).[15]

On the basis of the band position of the monomer conformers, the B18C6-$(H_2O)_1$ cluster seems to have the origin band at a frequency higher than those of the B18C6 monomers. That is, band A may appear via solvation of one water molecule to the B18C6 monomer that provides the 35167 cm^{-1} band. Then, the amount of the blue shift is 86 cm^{-1}. For bands B and C, two of the three monomer conformers that show the bands around 35640 cm^{-1} are hydrated, and the origin bands are shifted to the blue by ~100 cm^{-1}. Such a blue shift by hydration is characteristic of benzene molecules substituted by methoxy groups, which act as acceptors of hydrogen bond. The origin band of MB is blue-shifted by 118 cm^{-1} from monomer to monohydrated complex.[14] In the case of DMB, the origin is shifted to the blue by 127 cm^{-1} by hydration of one water molecule.[13] Thus, the amount of the blue shift of MB and DMB by hydration is comparable to those estimated for B18C6, and it is quite probable that one of two OH groups in B18C6-$(H_2O)_1$ is hydrogen-bonded to the oxygen atoms near the benzene ring.

In order to examine the ether ring conformation and hydration of B18C6 theoretically, we carried out density functional theory calculations for B18C6 and B18C6-$(H_2O)_1$ at the B3LYP/6-31+G* level of theory. Although B18C6 may have a variety of conformers originating from e.g. the dihedral angle of an –O–C–C–O–

segment, we found four stable conformations of the B18C6 monomer by the geometry optimization. The structures are shown in Fig. 4 with the total energy relative to that of the most stable structure. The most stable structure of the B18C6 monomer (conformer **I**) belongs to C_2 symmetry. The second lowest-energy structure (conformer **II**) also has a C_2 form, in which the O_7–C_8–C_9–O_{10} segment has a *trans* configuration. In these C_2 structures, the C_{15}, O_{16}, C_{17}, C_{18}, O_1 and C_2 atoms are located almost on the same plane. For conformer **IV**, the ring part has a D_{3d}-like structure, which is similar to 18-crown-6-ether.[11] In this form, the C_{15}, O_{16}, C_{17}, C_{18}, O_1 and C_2 atoms are no longer located on the same plane. In the case of conformer **III**, most of the configurations are similar to those of **IV**, but the noticeable difference between **III** and **IV** is that the O_1–C_2–C_3–O_4 part of **III** has a dihedral angle of ~60 degree, whereas that of **IV** is about –60 degree. It is not possible to give unambiguous assignment to the four B18C6 conformations existing in the jet on the basis of the present calculation, because we may have lost other stable structures of B18C6 in the calculation. However, these representative conformations in Fig. 4, especially **I** and **II**, well show the ring form characteristic of B18C6; the O_{16}, C_{17}, C_{18} and O_1 atoms prefer to be located on the same plane to keep the π-orbital clouds as large as possible around the benzene ring.

In the beginning of the geometry optimization of B18C6-$(H_2O)_1$, we have considered that a water molecule can be bound to several possible sites of the B18C6 monomers shown in Fig. 4. As a result, eight stable structures have been found for B18C6-$(H_2O)_1$, which are shown in Fig. 5. In the notation for the structures of B18C6-$(H_2O)_1$, the first Roman numeral presents the conformation of the B18C6 part, and the second number is for identifying the order of stability in the same ring

conformer. The total energy relative to that of the most stable isomer (**I-1**) is listed in Table 2. Here, it is again to be noted that there must be other B18C6-$(H_2O)_1$ isomers not found in the present calculation. In spite of the incompleteness for the search of the potential energy surface of B18C6-$(H_2O)_1$, we have to mention that a significant number of initial geometries are led to these eight isomers in the course of geometry optimization. The most stable structure is **I-1**; one of the two OH groups is bonded to the O_7 atoms, and the other OH bond points at the middle of the O_1 and O_{16} atoms that are connected to the benzene ring. The latter type of hydration is characteristic of benzo-crown ethers, and is not found for 18-crown-6-ether.[11] Among the eight structures of B18C6-$(H_2O)_1$, only isomer **I-3** has a single O–H···O hydrogen bond between B18C6 and water. However, this is the most unstable among the eight isomers. Isomers other than **I-3**, **III-2** and **IV-2** have a hydrogen bond at the O_1 and/or O_{16} atoms. On the basis of the blue shift of the origin band by hydration, we consider only the isomers (**I-1**, **I-2**, **II-1**, **III-1** and **IV-1**) having a hydrogen bond at the oxygen atoms near the benzene ring.

As seen in Fig. 3, the frequencies of the OH bands are similar among the three B18C6-$(H_2O)_1$ clusters. Therefore, it seems to be difficult to give a definitive assignment of observed B18C6-$(H_2O)_1$ to the calculated structures on the basis of the small frequency change. However, the observed IR spectra display small but noticeable difference in the band positions from each other. For example, the symmetric OH band is shifted to the low frequency from 3573 to 3564 cm^{-1} from bands A to C, and also the asymmetric OH band is shifted from 3656 to 3634 cm^{-1}. The amount of the shift for the asymmetric OH band (22 cm^{-1}) is larger than that for the symmetric one (9 cm^{-1}). For the OH stretching vibration in the O–H···O hydrogen

bonding system, there is a relationship between the hydrogen-bond strength and the frequency shift, which is typically referred to as the Badger-Bauer rule.[16] Following this rule, we can say that the B18C6-$(H_2O)_1$ isomer giving the IR spectrum in Fig. 3a has a hydrogen bond weaker than the isomer of the spectrum in Fig. 3c.

Table 2 lists the frequencies of the symmetric and asymmetric OH stretching vibrations of water of the B18C6-$(H_2O)_1$ isomers, where the calculated frequencies are corrected by a scaling factor of 0.9744. Figure 6 displays relationship between geometrical parameters and the OH stretching frequencies of the water molecule. The horizontal axis in Fig. 6a is the interatomic distance between the hydrogen atoms of the water and the proton-accepting oxygen atoms, and that in Fig. 6b is the O–H···O angle. For isomers **I-1** and **IV-1**, we use the averaged parameters for three values; for example, the interatomic distance of **I-1** is derived by the average of the H···O_1, H···O_{16}, and H···O_7 distances. From Figs. 6a and 6b, one can classify the B18C6-$(H_2O)_1$ isomers into two groups. One group consists of isomers **I-1** and **IV-1**; the H···O distances is around 2.32 Å, and the O–H···O angle is ~152 degree. The other group consists of **I-2**, **II-1** and **III-1**; the distance (~2.02 Å) is shorter than that of the former group, and the angle (~173 degree) is larger. We expect that the shorter O–H···O distance and the larger O–H···O angle suggest stronger hydrogen bond, and the OH stretching frequencies of these two groups well reflect this expectation. Isomers **I-1** and **IV-1** have the symmetric and asymmetric OH stretch bands at 3584 and 3681 cm^{-1} in average, which are higher than the frequencies of the corresponding bands of **I-2**, **II-1** and **III-1** (3571 and 3649 cm^{-1} in average). Isomer **I-1** is the most stable isomer, and isomer **IV-1** is the second most stable one among the eight isomers. The stability of these isomers mainly originates from their unique hydration manner. That is, one OH group

is bonded to both the O_1 and O_{16} atoms. Although the frequency shift of the OH vibration due to the hydrogen bond formation is small, the water molecule may be strongly bound by the cooperation of two hydrogen bonds with O_1 and O_{16}. Therefore, B18C6-$(H_2O)_1$ providing band A in the LIF spectra and the IR spectrum in Fig. 3a can originate from a structure like **I-1** or **IV-1**. As mentioned previously, the B18C6-$(H_2O)_1$ isomer of band A may have a planar nature around the benzene ring. On the basis of this consideration, the most probable isomer of band A is isomer **I-1**, which has C_2 symmetry in the ether ring. As can be seen in Fig. 6, the difference of the averaged frequency between the two groups is 13 cm^{-1} and 37 cm^{-1} for the symmetric and asymmetric OH vibrations, respectively. The amount of the difference is comparable to the difference of the band position observed in Figs. 3a and 3c (9 and 22 cm^{-1}). Therefore, the B18C6-$(H_2O)_1$ isomer corresponding to band C in the LIF spectra and the IR spectrum in Fig. 3c can be assigned to one of the isomers of **I-2**, **II-1** and **III-1**, in which one of the OH groups is bonded to the O_1 atom. The B18C6-$(H_2O)_1$ isomer corresponding to band B in the LIF spectra and the IR spectrum in Fig. 3b may have an intermediately strong hydrogen bond, although we cannot give any specific structure at present.

3.3. Hydration of DB18C6

DB18C6 has two benzene rings on the opposite sides of the crown ether ring. Therefore, the DB18C6 monomer may have a higher symmetry than B18C6. In addition, the two aromatic rings further reduce the number of the ring conformation of DB18C6 compared to B18C6 because of the preference of the planar configuration around the two aromatic rings. Figure 7 shows LIF spectra of DB18C6 observed (a)

without and (b) with water vapor in He carrier gas. Also shown are the UV-UV hole-burning spectra. Similar to B18C6, bands marked by dots are assignable to the origin bands of different conformers of bare DB18C6, which is confirmed by UV-UV and IR-UV spectra. The IR-UV spectra of these bands show no OH stretching band, and their UV-UV hole-burning spectra display different spectral features from each other. From the measurement of IR-UV spectra, only band D can be ascribed to the DB18C6-$(H_2O)_1$ cluster. The band marked by the asterisk is due to a hydrated cluster with more than one water molecule, because the IR-UV spectrum of this band has more than two bands of the OH stretching vibration. By comparing the LIF spectra in Figs. 2a and 7a, we can suggest that B18C6 produces more hydrated clusters than DB18C6 without the additional water, which means that hydration to B18C6 is more efficient than to DB18C6. This is partly due to the structural constraint of DB18C6 in which the ether ring is quite rigid due to the two benzene rings so that it cannot change the configuration easily as suitable for water solvation.

Figure 8 shows the IR-UV dip spectrum measured by monitoring band D. There are two bands in the OH stretching region, suggesting that band D originates from DB18C6-$(H_2O)_1$. The frequencies of these bands are similar to those of B18C6-$(H_2O)_1$ in Fig. 3. Therefore, the low- and high-frequency bands in Fig. 8 can be ascribed to the symmetric and asymmetric stretching vibrations of the water molecule bonded to the ether oxygen atoms. As seen in the LIF spectra in Fig. 7, band D is located on the blue side of the monomer bands, suggesting that the water molecule is bonded to the oxygen atoms near the benzene rings, similar to the case of B18C6-$(H_2O)_1$. In addition, we can assume that the OH groups of water are not bound to the neighboring oxygen atoms directly connected by the $–CH_2–CH_2–$ chain. We

then carried out the geometry optimization and vibrational analysis of DB18C6 and DB18C6-$(H_2O)_1$. For bare DB18C6, we obtained four stable structures. Figure 9 shows (a) the lowest and (b) the second lowest energy conformers of DB18C6. The lowest energy conformer of DB18C6 has a C_{2v} structure, which can be called "boat" type. The second one has a "chair" type structure. The energy difference between these structures is 739 cm^{-1}. Figure 9c shows the lowest-energy structure of the DB18C6-$(H_2O)_1$ cluster. In this isomer, the two OH groups are hydrogen bonded to the middle of (O_{10}, O_{13}) and (O_2, O_3). This structure is consistent with that predicted by the LIF and IR spectra, and similar to the most stable structure of B18C6-$(H_2O)_1$. Therefore, this type of hydration, in which the two oxygen atoms near the benzene ring become acceptors of the hydrogen bond, is characteristic of benzo-crown ethers. The IR spectrum calculated for B18C6-$(H_2O)_1$ in Fig. 9c has the symmetric and asymmetric OH bands at 3597 and 3689 cm^{-1}. These calculated frequencies are similar to those observed in the IR spectrum in Fig. 8 (3580 and 3648 cm^{-1}, respectively). Therefore, we can conclude that DB18C6-$(H_2O)_1$ providing band D in the LIF spectra and the IR-UV spectrum in Fig. 8 has a form like the structure in Fig. 9c.

4. Conclusion

LIF spectroscopy, and UV-UV and IR-UV double-resonance spectroscopy have been applied to monomers and hydrates of benzo-18-crown-6 (B18C6) and dibenzo-18-crown-6 (DB18C6) under the jet-cooled condition. We found four conformers for bare B18C6 and three isomers for B18C6-$(H_2O)_1$. IR-UV spectra of B18C6-$(H_2O)_1$ show two bands around 3570 and 3640 cm^{-1}. These bands are assigned

to the symmetric and asymmetric OH stretching vibrations of water forming a double proton-donor type (bidentate) hydration to oxygen atoms of the ether ring. The blue shift of the origin band from B18C6 to B18C6-$(H_2O)_1$ suggests that one of the water OH is bonded to the oxygen atoms near the benzene ring in B18C6-$(H_2O)_1$. In the case of DB18C6, there are two conformers for bare DB18C6 and there is a single isomer for DB18C6-$(H_2O)_1$. The IR-UV spectrum of DB18C6-$(H_2O)_1$ shows two bands at 3580 and 3648 cm^{-1}. These bands are also ascribed to the symmetric and asymmetric OH stretching vibrations of a bidentate water. A common feature of B18C6-$(H_2O)_1$ and DB18C6-$(H_2O)_1$ is that the water OH is bound to the oxygen atoms near the benzene ring. This type of hydration is due to the planar nature of the –O–C–C–O– frame in the benzene rings as supposed by the effective π conjugation. For the future work, we extend our study to the larger size hydrated clusters, B18C6-$(H_2O)_{n>1}$ and DB18C6-$(H_2O)_{n>1}$, which are in progress.

Acknowledgment

We gratefully acknowledge valuable discussion with Dr. S. Xantheas in Pacific Northwest National Laboratory. This work is supported by Grant-in-Aids for Scientific Research (#18205003 and #18685001) by the Ministry of Education, Science, Sports, and Culture, Japan.

Table 1. Band position of the origin band for B18C6 and DB18C6.

Position (cm^{-1})	Assignment[a]
35167	B18C6
35628	B18C6
35659	B18C6
35666	B18C6
35253	B18C6-$(H_2O)_1$
35758	B18C6-$(H_2O)_1$
35771	B18C6-$(H_2O)_1$
35598	DB18C6
35688	DB18C6
35777	DB18C6-$(H_2O)_1$

[a]All the bands in this table are assigned to the different conformers or isomers by UV-UV and IR-UV double-resonance spectroscopy.

Table 2. Total energies (cm^{-1}), and frequencies (cm^{-1}) and IR intensities (km/mol) of the OH stretching vibrations for optimized structures of the B18C6-$(H_2O)_1$ cluster.

Isomer	Total Energy (cm^{-1})[a]	OH Stretching Frequency (cm^{-1})[b]	
		Symmetric	Asymmetric
I-1	0	3576 (117)	3684 (232)
IV-1	38	3592 (59)	3687 (277)
III-1	224	3570 (93)	3653 (392)
IV-2	294	3586 (91)	3673 (268)
I-2	410	3573 (132)	3646 (322)
II-1	462	3569 (104)	3649 (299)
III-2	1074	3570 (99)	3652 (329)
I-3	1498	3496 (368)	3719 (94)

[a]Total energy relative to that of the most stable structure (isomer **I-1**). These values are corrected by the zero-point vibrational energy.
[b]Calculated frequencies are multiplied by a scaling factor of 0.9744. This factor is determined so as to reproduce the OH stretching frequency of phenol monomer at the same calculation level (B3LYP/6-31+G*).

Figure captions

Figure 1. LIF spectra of (a) B18C6 and (b) DB18C6 in the 35100–36900 cm^{-1} region.

Figure 2. LIF spectra of B18C6 observed (a) without and (b) with additional water in the jet sample. UV-UV hole burning spectra obtained by fixing probe frequency to the band at (c) 35167, (d) 35628, (e) 35659, and (f) 35666 cm^{-1}, respectively. In (b), water vapor was added by flowing the He carrier gas over ice. Bands marked by dots are due to B18C6 monomer, by alphabet are due to B18C6-$(H_2O)_1$, and by asterisks are due to B18C6-$(H_2O)_{n>1}$.

Figure 3. IR-UV spectra of B18C6-$(H_2O)_1$ observed by monitoring (a) band A, (b) band B and (c) band C in the LIF spectra of B18C6.

Figure 4. Optimized structures of the B18C6 monomer at the B3LYP/6-31+G* level of theory. Energies in cm^{-1} are the total energies relative to that of the most stable conformer (**I**), which are corrected by the zero-point vibrational energy.

Figure 5. Optimized structures of B18C6-$(H_2O)_1$ at the B3LYP/6-31+G* level of theory. Roman numeral in the notation shows the ether ring conformation of each isomer (see also Fig. 4). Energies in cm^{-1} are the total energies relative to that of the most stable isomer (**I-1**). The values are corrected by the zero-point vibrational energy.

Figure 6. Relationship between the frequencies of the symmetric (closed circles) and asymmetric (open circles) OH stretching vibrations of water and the geometric parameters for the optimized structures of B18C6-$(H_2O)_1$. The frequencies are plotted as a function of (a) H···O distance and (b) O–H···O angle in the O–H···O hydrogen bond. The calculated frequencies are multiplied by the scaling factor of 0.9744.

Figure 7. LIF spectra of DB18C6 observed (a) without and (b) with additional water in the jet sample. UV-UV hole burning spectra obtained by fixing probe frequency to band at (c) 35598, and (d) 35688 cm^{-1}, respectively. The water vapor was added by flowing the He carrier gas over ice.

Figure 8. IR-UV spectrum of DB18C6-$(H_2O)_1$ observed by monitoring band D in the LIF spectra of DB18C6.

Figure 9. Optimized structures of the DB18C6 monomer and the DB18C6-$(H_2O)_1$ complex at the B3LYP/6-31+G* level of theory. Energies in cm^{-1} are the total energies of the DB18C6 monomer relative to that of the most stable conformer. The values are corrected by the zero-point vibrational energy.

References

[1] C. J. Pedersen, *Science*, 1988, **241**, 536.

[2] D. Bright and M. R. Truter, *J. Chem. Soc. (B)*, 1970, 8, 1544; D. Live and S. I. Chan, *J. Am. Chem. Soc.*, 1976, **98**, 3769; M. J. Wilson, R. A. Pethrick, D. Pugh and M. Saiful Islam, *J. Chem. Soc. Faraday Trans.*, 1997, **93**, 2097; S. Krongsuk, T. Kerdcharoen and S. Hannongbua, *J. Phys. Chem. B*, 2003, **107**, 4175; S. Krongsuk, T. Kerdcharoen, M. Kiselev and S. Hannongbua, *Chem. Phys.*, 2006, **324**, 447.

[3] C. J. Pedersen, *J. Am. Chem. Soc.*, 1967, **89**, 2495; C. J. Pedersen, *J. Am. Chem. Soc.*, 1967, **89**, 7017.

[4] J. S. Benco, H. A. Nienaber, K. Dennen and W. G. McGimpsey, *J. Photochem. Photobiol. A: Chemistry*, 2002, **152**, 33.

[5] D. J. Cram, R. A. Carmack and R. C. Helgeson, *J. Am. Chem. Soc.*, 1988, **110**, 571.

[6] T. Ebata, T. Hashimoto, T. Ito, Y. Inokuchi, F. Altunsu, B. Brutschy and P. Tarakeshwar, *Phys. Chem. Chem. Phys.*, 2006, **8**, 4783; Y. Inokuchi, Y. Kobayashi, T. Ito and T. Ebata, *J. Phys. Chem. A*, 2007, **111**, 3209.

[7] Gaussian 03, Revision B.05, M. J. Frisch, G. W. Trucks, H. B. Schlegel, G. E. Scuseria, M. A. Robb, J. R. Cheeseman, J. A. Montgomery, Jr., T. Vreven, K. N. Kudin, J. C. Burant, J. M. Millam, S. S. Iyengar, J. Tomasi, V. Barone, B. Mennucci, M. Cossi, G. Scalmani, N. Rega, G. A. Petersson, H. Nakatsuji, M. Hada, M. Ehara, K. Toyota, R. Fukuda, J. Hasegawa, M. Ishida, T. Nakajima, Y. Honda, O. Kitao, H. Nakai, M. Klene, X. Li, J. E. Knox, H. P. Hratchian, J. B. Cross, C. Adamo, J. Jaramillo, R. Gomperts, R. E. Stratmann, O. Yazyev, A. J. Austin, R. Cammi, C. Pomelli, J. W. Ochterski, P. Y. Ayala, K. Morokuma, G. A. Voth, P. Salvador, J. J. Dannenberg, V. G. Zakrzewski, S.

Dapprich, A. D. Daniels, M. C. Strain, O. Farkas, D. K. Malick, A. D. Rabuck, K. Raghavachari, J. B. Foresman, J. V. Ortiz, Q. Cui, A. G. Baboul, S. Clifford, J. Cioslowski, B. B. Stefanov, G. Liu, A. Liashenko, P. Piskorz, I. Komaromi, R. L. Martin, D. J. Fox, T. Keith, M. A. Al-Laham, C. Y. Peng, A. Nanayakkara, M. Challacombe, P. M. W. Gill, B. Johnson, W. Chen, M. W. Wong, C. Gonzalez and J. A. Pople, Gaussian, Inc., Pittsburgh PA, 2003.

[8] T. Iimori and Y. Ohshima, *J. Chem. Phys.*, 2002, **117**, 3656.

[9] J. B. Hopkins, D. E. Powers and R. E. Smalley, *J. Chem. Phys.*, 1980, **72**, 5039.

[10] H. Matsuura, Md. Ruhul Matin and K. Ohno, *Chem. Lett.*, 2003, **32**, 122; Md. Ruhul Matin, Y. Katsumoto, H. Matsuura and K. Ohno, *J. Phys. Chem. B*, 2005, **109**, 19704.

[11] K. Fukuhara, M. Tachikake, S. Matsumoto and H. Matsuura, *J. Phys. Chem.*, 1995, **99**, 8617.

[12] Z. S. Nickolov, N. Goutev and H. Matsuura, *J. Phys. Chem. A*, 2001, **105**, 10884.

[13] J. T. Yi, J. W. Ribblett and D. W. Pratt, *J. Phys. Chem. A*, 2005, **109**, 9456.

[14] B. Reimann, K. Buchhold, H.-D. Barth, B. Brutschy, P. Tarekeshwar and K.-S. Kim, *J. Chem. Phys.*, 2002, **117**, 8805.

[15] B. C. Dian, A. Longarte, S. Mercier, D. A. Evans, D. J. Wales and T. S. Zwier, *J. Chem. Phys.*, 2002, **117**, 10688.

[16] S. Scheiner, in *HYDROGEN BONDING*, Oxford Univ. Press, New York, 1997, pp. 140.

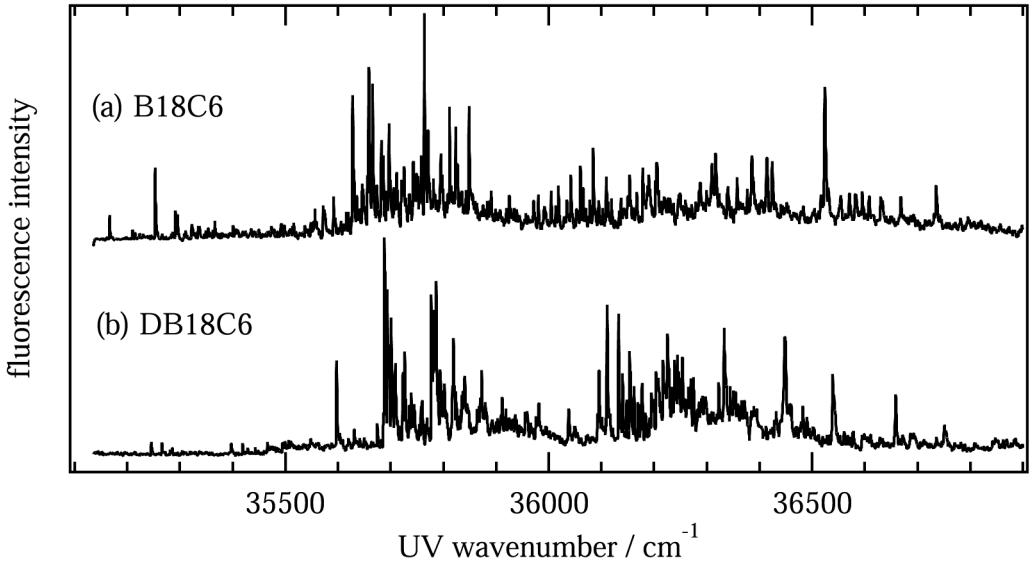

Fig. 1. Kusaka et al.

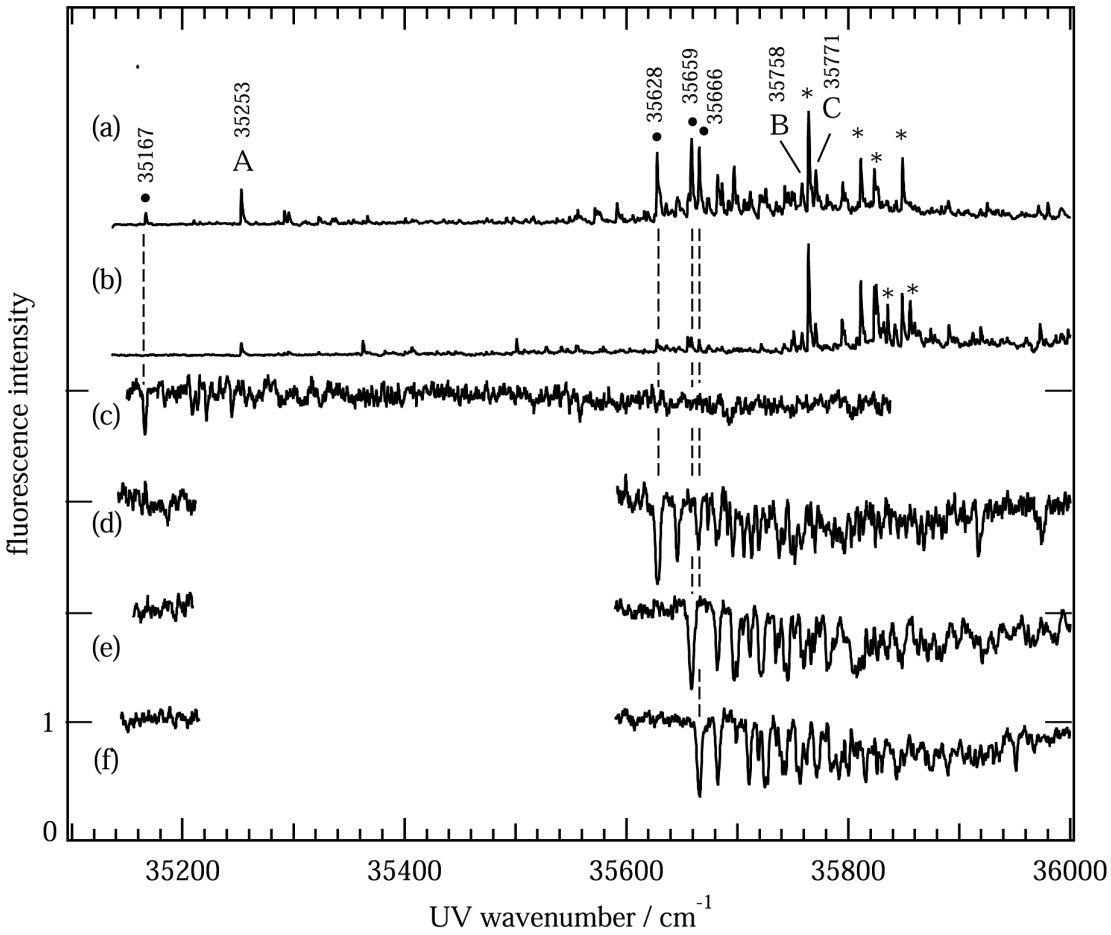

Fig. 2. Kusaka et al.

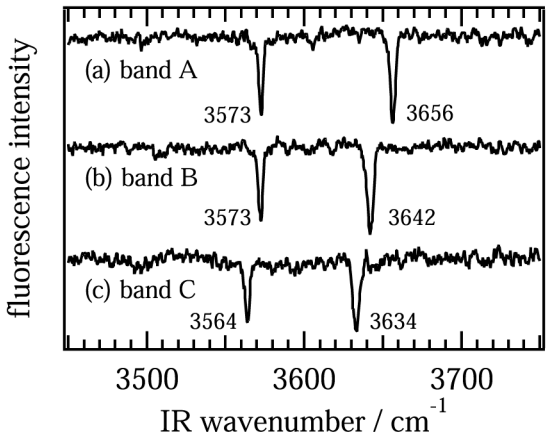

Fig. 3. Kusaka et al.

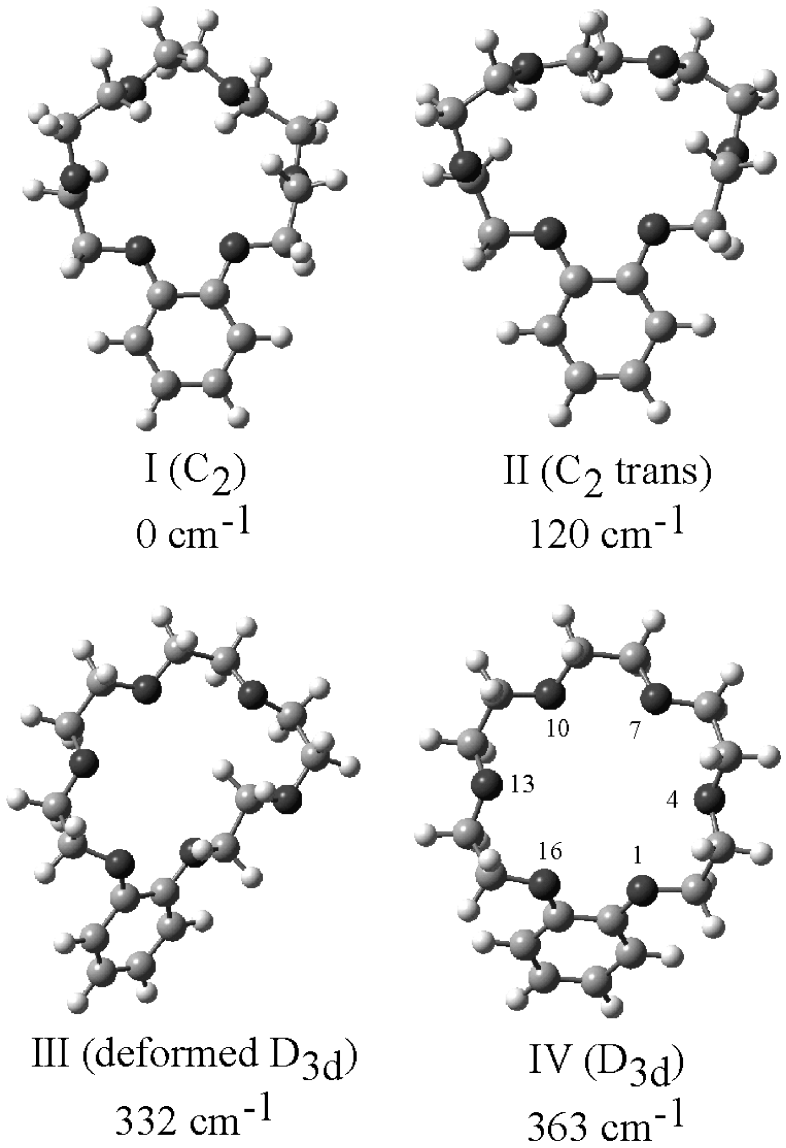

Fig. 4. Kusaka et al.

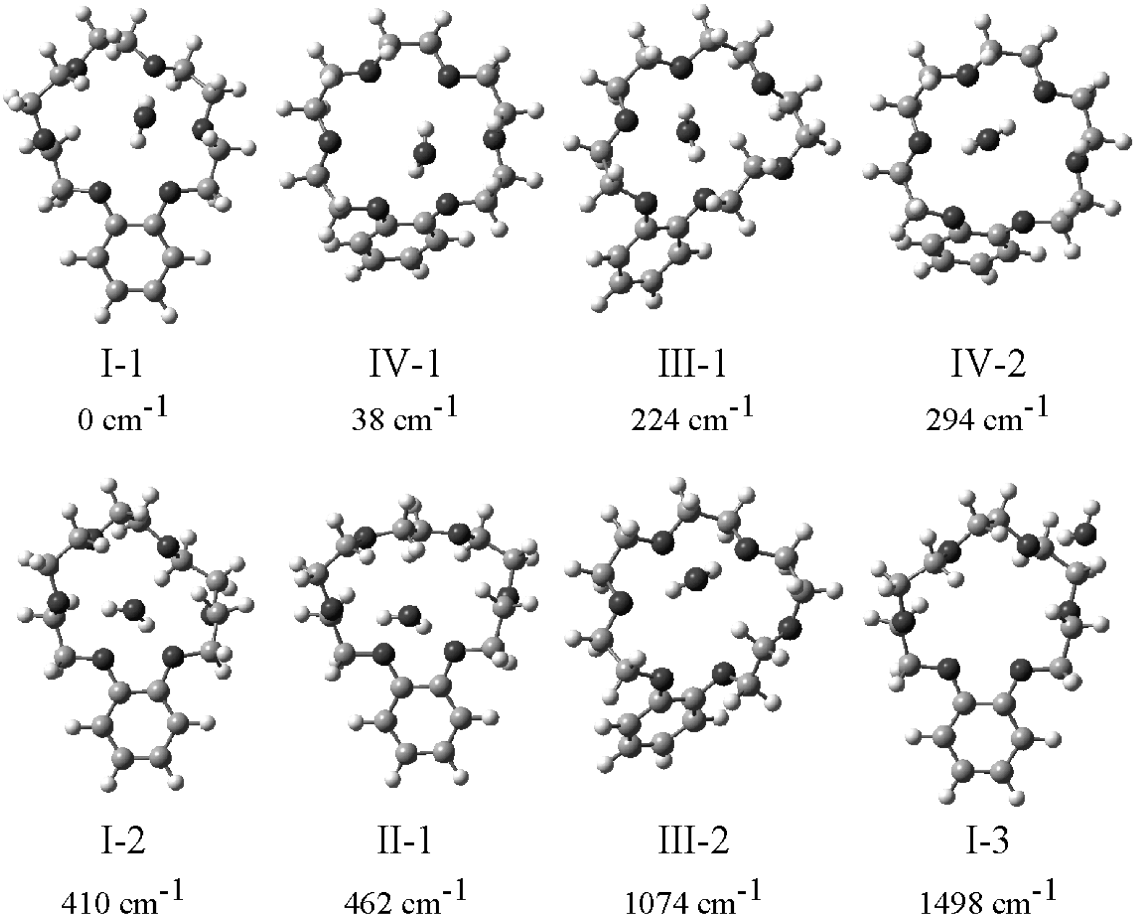

Fig. 5. Kusaka et al.

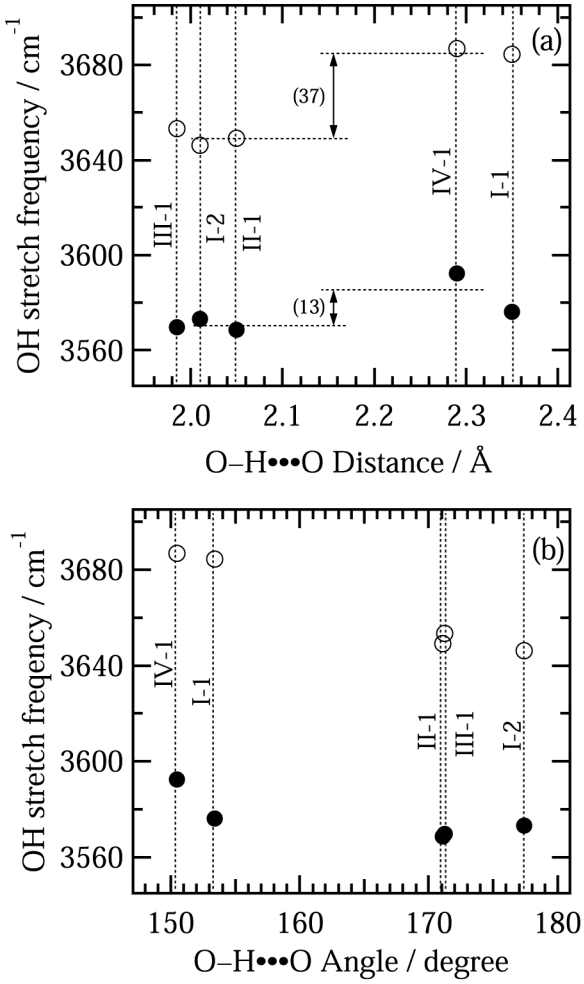

Fig. 6. Kusaka et al.

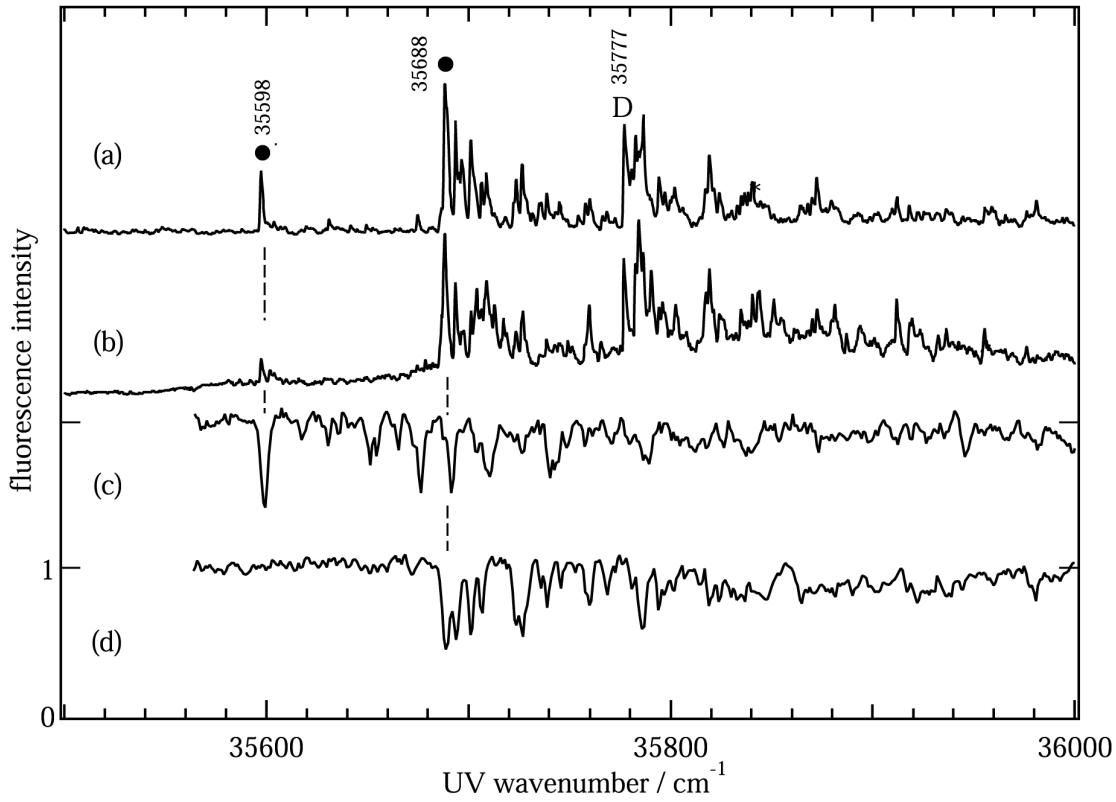

Fig. 7. Kusaka et al.

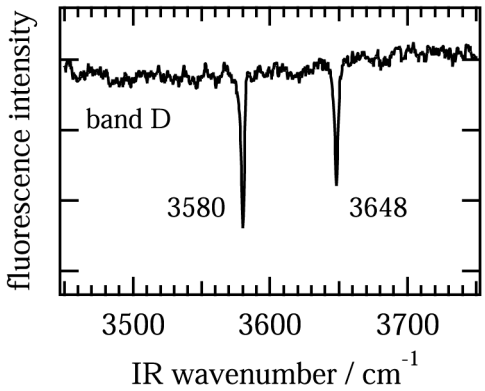

Fig. 8. Kusaka et al.

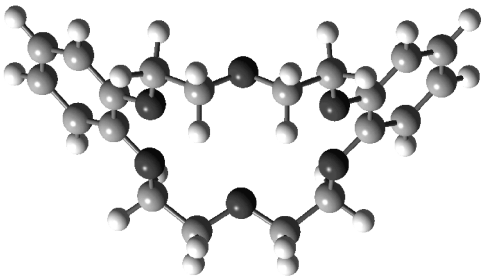

(a) boat

0 cm^{-1}

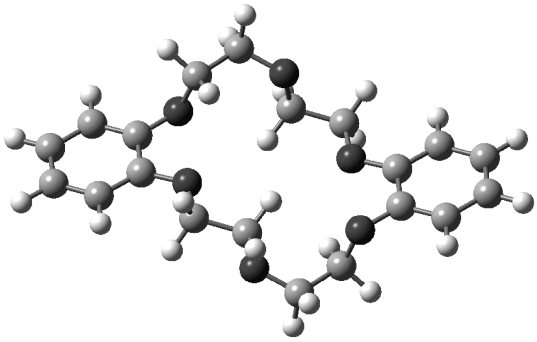

(b) chair

739 cm^{-1}

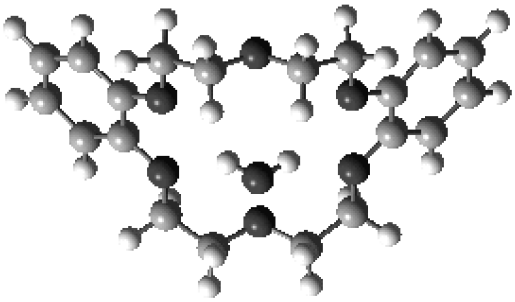

(c) boat + H_2O

Fig. 9. Kusaka et al.